

Monte Carlo investigation of terahertz plasma oscillations in ultrathin layers of n -type $\text{In}_{0.53}\text{Ga}_{0.47}\text{As}$

J.-F. Millithaler^{a)} and L. Reggiani

Dipartimento di Ingegneria dell'Innovazione and CNISM, Università del Salento, Lecce, Salento 73100, Italy

J. Pousset, L. Varani, and C. Palermo

Institut d'Electronique du Sud, UMR CNRS 5214, Université Montpellier II, place Bataillon, 34095 Montpellier Cedex 5, France

W. Knap

Groupe d'Etude des Semiconducteurs, UMR CNRS 5650, Université Montpellier II, place Bataillon, 34095 Montpellier Cedex 5, France

J. Mateos, T. González, S. Perez, and D. Pardo

Departamento de Física Aplicada, Universidad de Salamanca, Pza. Merced s/n 37008 Salamanca, Spain

(Received 22 October 2007; accepted 3 December 2008; published online 30 January 2008)

By numerical simulations we investigate the dispersion of the plasma frequency in a n -type $\text{In}_{0.53}\text{Ga}_{0.47}\text{As}$ layer of thickness W and submicron length at $T=300$ K. For $W=100$ nm and carrier concentrations of 10^{16} – 10^{18} cm^{-3} the results are in good agreement with the standard three-dimensional (3D) expression of the plasma frequency. For $W \leq 10$ nm the results exhibit a plasma frequency that depends on L , thus implying that the oscillation mode is dispersive. The corresponding frequency values are in good agreement with the two-dimensional (2D) expression of the plasma frequency obtained for a ballistic regime within the in-plane approximation for the electric field. A region of cross over between the 2D and 3D behaviors of the plasma frequency is evidenced for $W > 10$ nm. © 2008 American Institute of Physics. [DOI: 10.1063/1.2837183]

Terahertz radiation has potential applications in different domains, such as broadband communications, high-resolution spectroscopy, environment monitoring, biomedical testing, etc.^{1,2} As a consequence, the realization of a room-temperature operating, compact, and affordable, solid-state terahertz radiation source with coherent, powerful, and tunable characteristics is a mandatory issue. If terahertz radiation generation and detection can be envisaged by using optical or electronic systems, then one of the most promising strategies lies in the plasmonic approach. In this framework, Dyakonov and Shur have considered, through an analytical approach, the case of a two-dimensional electron layer constituted by the ungated channel of a nanometric transistor.³ The electron gas was assumed as highly concentrated but nondegenerate, and supposed to undergo only long-range electron-electron interaction. By making a small signal analysis of the self-consistent set of coupled equations within the in-plane field approximation, the electron gas is found to behave as the support of plasma waves whose propagation velocity can be greater than the electron drift velocity.⁴ Through the oscillations of the plasma, nanometric high electron mobility transistors have been suggested as possible emitters and detectors of electromagnetic radiation in the terahertz range.^{5–7} The aim of this work is to investigate the same problem from a microscopic point of view, thus, testing the limits of applicability of the analytical approach. To this purpose, we consider a n -type $\text{In}_{0.53}\text{Ga}_{0.47}\text{As}$ layer embedded in a symmetric dielectric and investigate the plasma frequency characteristics by analyzing the frequency spectrum of voltage fluctuations obtained from a Monte Carlo (MC)

simulator coupled with a two-dimensional (2D) Poisson solver.

We recall that the plasma wave of a 2D sheet of electrons moving under ballistic conditions, within the in-plane field approximation for the solution of the Poisson equation, leads to a dispersive 2D plasma frequency³

$$\omega_p^{2D} = \sqrt{\frac{e^2 n_0^{2D} k}{2m_0 m \epsilon_0 \epsilon_{\text{diel}}}}, \quad (1)$$

where k is the wavevector, m_0 and m are the free and effective electron masses, respectively, n_0^{2D} is the average 2D carrier concentration, ϵ_{diel} the relative dielectric constant of the outside dielectric, and ϵ_0 is the vacuum permittivity. We notice that the 2D plasma frequency depends on the relative dielectric constant of the external dielectric, and that charge image effects are neglected. Plasma waves also exist in bulk and their three dimensional (3D) dispersionless frequency is

$$\omega_p^{3D} = \sqrt{\frac{e^2 n_0^{3D}}{m_0 m \epsilon_0 \epsilon_{\text{mat}}}}, \quad (2)$$

where n_0^{3D} is the 3D average carrier concentration and ϵ_{mat} is the relative dielectric constant of the bulk material.

The numerical solution of this problem is carried out by using a microscopic MC approach coupled with a two-dimensional Poisson solver.^{5,8} The parameters of the microscopic model are those of Ref. 9. By evaluating the fluctuations of the voltage in the center of the device under test, the spectral density of this quantity is extracted and the plasma frequency determined from the characteristic peak exhibited by the spectrum. To study the plasma oscillations in the 3D and 2D cases, we simulate a bar of $\text{In}_{0.53}\text{Ga}_{0.47}\text{As}$ of length L in the range of 0.1–1 μm for different thicknesses W and

^{a)}Electronic mail: jf.millithaler@unile.it.

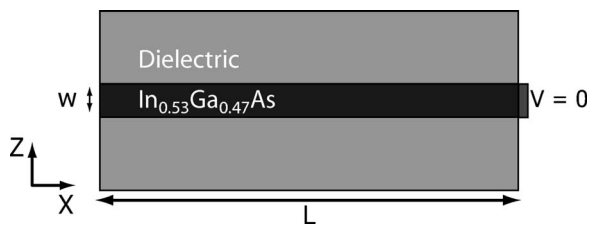


FIG. 1. Schematic of the device studied within the Monte Carlo simulation. The free charge is present only in the bar of length L along the x direction and thickness W along the z direction. The terminal at the right hand side is kept at zero voltage and is connected to an ideal thermal reservoir of electrons which are injected at a constant rate into the bar. Carriers are reflected at the boundaries between the bar and the dielectric as well as when reaching the open terminal at the left hand side.

carrier concentrations, with one terminal of the bar connected with an infinite reservoir of electrons at thermal equilibrium and the other terminal being open circuited. The bar is surrounded by a perfect dielectric (Fig. 1) (here taken as the vacuum) $10\ \mu\text{m}$ wide in the upper and lower regions of the bar, where the 2D Poisson equation in the xz plane is solved to account for the fringing of the external electric field. For a comparative analysis between numerical simulations and analytical results, we take $k=2\pi/L$ and $n_0^{2D}=n_0^{3D}\cdot W$. The simulated structure, which is depicted in Fig. 1, represents a simplified version of the transistor channel for the ungated case. The time and space discretizations take typical values of $0.2\text{--}10$ fs for the time step, $0.1\text{--}2$ nm for the spatial scale of the bar, 500 nm for the spatial scale of the dielectric. Typically there are 80 carriers inside a mesh of the bar, found to provide a correct solution of the Poisson equation.

We start by considering the case of a channel of thickness $W=100$ nm. Figure 2 reports the spectral density of voltage fluctuation, for a length of the device $L=0.1\ \mu\text{m}$ and for a free electron density $n_0^{3D}=10^{18}\ \text{cm}^{-3}$, which corresponds to the autocorrelation function of voltage fluctuations given in the figure inset. We can observe that the amplitude of the autocorrelation function at short times decreases exponentially with an oscillation superimposed to the zero value. Accordingly, the spectral density exhibits a well defined peak at the frequency $f=10$ THz, in good agreement with the expected 3D plasma value of Eq. (4). Figure 3 reports the peak frequency $f_p=\omega/(2\pi)$ as a function of the

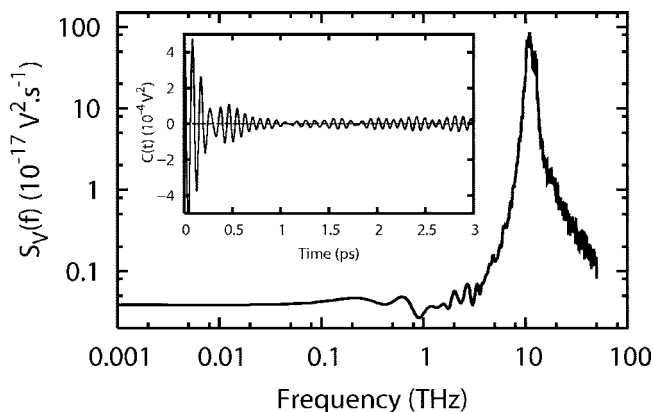


FIG. 2. Spectral density of voltage fluctuations as a function of frequency for a $\text{In}_{0.53}\text{Ga}_{0.47}\text{As}$ channel of thickness $W=100$ nm with $n_0^{3D}=10^{18}\ \text{cm}^{-3}$ and $L=0.1\ \mu\text{m}$ at room temperature. The insert reports the corresponding autocorrelation function of voltage fluctuations.

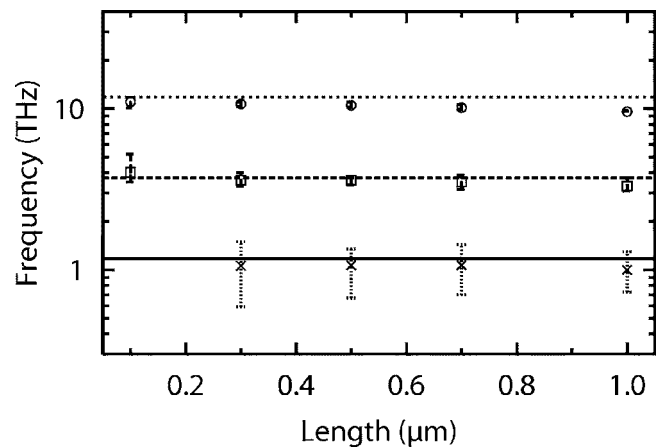


FIG. 3. Plasma frequency as a function of the channel length for a thickness $W=100$ nm and for free electron densities $n_0^{3D}=10^{16}\ \text{cm}^{-3}$ (crosses and continuous lines), $n_0^{3D}=10^{17}\ \text{cm}^{-3}$ (squares and dashed lines), $n_0^{3D}=10^{18}\ \text{cm}^{-3}$ (circles and dotted lines). Lines correspond to Eq. (2) and symbols with errorbar exceeding the size of the symbol refer to Monte Carlo simulations.

device length for different values of the carrier concentration. We remark that the peak frequency is greater for higher values of the electron density and that, for a given value of the electron density, is nearly constant with the channel length. Indeed, this situation corresponds to the case of a 3D electron gas case where the plasma frequency associated with voltage fluctuations exhibits an angular frequency ω_p^{3D} given by Eq. (2).

We then consider the case of a channel of thickness $W=1$ nm. The corresponding MC results for the frequency peak are reported in Fig. 4. We remark that, for a given value of the channel length, the peak frequency is still greater for higher concentrations. However, for a given value of the sheet electron density, the oscillation frequency decreases at increasing sample lengths in close agreement with the prediction of the 2D analytical theory. Here, by exploiting the predictivity of the analytical results quantum effects are disregarded. The results for the 1 and 100 nm thicknesses represent asymptotic behaviors of a 2D and 3D plasma and point to the existence of a cross over which cannot be predicted by the analytical theory. Accordingly, the cross-over

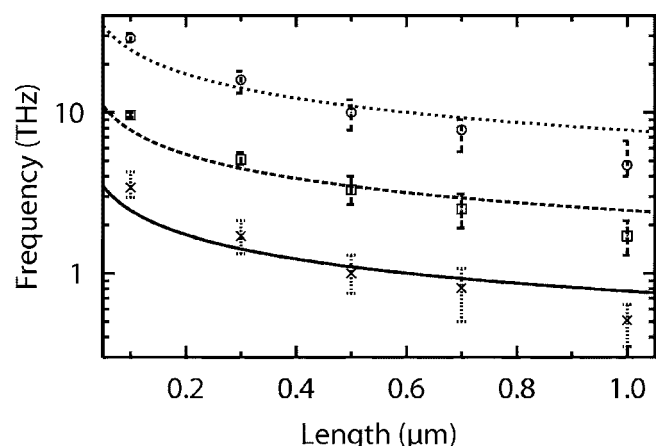


FIG. 4. Plasma frequency as a function of the channel length for a thickness $W=1$ nm and for free electron densities $n_0^{2D}=10^{10}\ \text{cm}^{-2}$ (crosses and continuous lines), $n_0^{2D}=10^{11}\ \text{cm}^{-2}$ (squares and dashed lines), $n_0^{2D}=10^{12}\ \text{cm}^{-2}$ (circles and dotted lines). Lines correspond to Eq. (1) and symbols with errorbar exceeding the size of the symbol refer to Monte Carlo simulations.

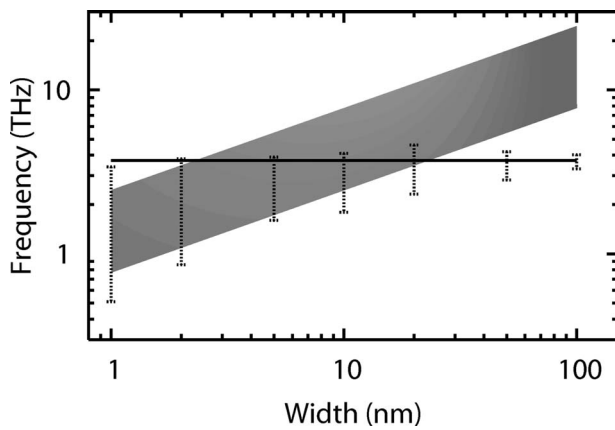


FIG. 5. Plasma frequency as a function of the channel width for an electron density $n_0^{3D} = 10^{17} \text{ cm}^{-3}$. The continuous line refers to the 3D of Eq. (2), the shaded region refers to the 2D of Eq. (1) covering the two cases of $L = 0.1\text{--}1 \mu\text{m}$, the dashed bars refers to Monte Carlo results covering the same two cases.

region has been investigated by simulating different thicknesses in the intermediate region of 10–50 nm. The results are summarized in Fig. 5. Here the plasma frequencies obtained by simulations are reported together with the theoretical values of Eqs. (2) and (3), for a 3D carrier concentration of 10^{17} cm^{-3} . We notice that the region of cross over is centered at about 10 nm, which compares well with the value of the 3D Debye length, $L_D = 14 \text{ nm}$. The analogous calculations carried out for a 3D carrier concentrations of 10^{18} cm^{-3} confirms the same trend.

In conclusion, from the calculation of the spectral density of voltage fluctuations we have investigated plasma oscillations in $\text{In}_{0.53}\text{Ga}_{0.47}\text{As}$ channels of different lengths, thicknesses, and carrier concentrations under thermal equilibrium conditions. The results of MC simulations show that

for thick channels, above 100 nm, 3D plasma oscillations appear and depend only on carrier concentration. By contrast, for thin channels below 100 nm, we have observed the transition from 3D to 2D plasma modes where the plasma frequency decreases with the length of the channel in close agreement with the analytical model.³ The simulations show (i) that the presence of scattering does not influence the value of the plasma frequency predicted by the ballistic theory and (ii) the existence of a cross over between the 2D and 3D behavior of the plasma frequency, which happens at width above about 10 nm.

The work was supported by CNRS-GDR and GDR-E projects Semiconductor sources and detectors of terahertz frequencies, Region Languedoc-Roussillon project Plateforme Technologique THz, Dirección General de Investigación (MEC, Spain), FEDER Project No. TEC2004-05231, and Consejera de Educación of Junta de Castilla y León (Spain) Project No. SA044A05.

¹D. Mittleman, M. Gupta, R. Neelamani, J. Baraniuk, R. Rudd, and M. Koch, *Appl. Phys. B: Lasers Opt.* **68**, 1085 (1999).

²D. L. Wollard, E. R. Brown, M. Pepper, and M. Kemp, *Proc. IEEE* **93**, 1722 (2005).

³M. Dyakonov and M. S. Shur, *Appl. Phys. Lett.* **87**, 111501 (2005).

⁴M. Dyakonov and M. Shur, in *TeraHertz Sources and Systems*, NATO Science Series, II. Mathematics, Physics and Chemistry, edited by M. E. Miles (Kluwer Academic, Boston, 2001), Vol. 27, pp. 187–207.

⁵J. Lusakowski, W. Knap, N. Dyakonova, L. Varani, J. Mateos, T. González, Y. Roelens, S. Bollaert, A. Cappy, and K. Karpierz, *J. Appl. Phys.* **97**, 064307 (2005).

⁶V. Ryzhii and M. S. Shur, *Jpn. J. Appl. Phys., Part 2* **45**, L1119 (2006).

⁷G. R. Aizin, D. V. Fateev, G. M. Tsybalov, and V. V. Popov, *Appl. Phys. Lett.* **91**, 163507 (2007).

⁸C. Jacoboni and P. Lugli, *The Monte Carlo Method for Semiconductor Device Simulation* (Springer, Wien, 1989).

⁹J. Mateos, T. González, D. Pardo, V. Hoël, and A. Cappy, *IEEE Trans. Electron Devices* **47**, 250 (2000).